
Unsupervised Structural-Counterfactual Generation under Domain Shift

Krishn V. Kher^{*1} Lokesh Badisa^{*1} K.V.D Sri Harsha^{†2} C.G Sowmya^{†2} SakethaNath Jagarlapudi¹

Abstract

Motivated by the burgeoning interest in cross-domain learning, we present a novel generative modeling challenge: generating counterfactual samples in a target domain based on factual observations from a source domain. Our approach operates within an unsupervised paradigm devoid of parallel or joint datasets, relying exclusively on distinct observational samples and causal graphs for each domain. This setting presents challenges that surpass those of conventional counterfactual generation. Central to our methodology is the disambiguation of exogenous causes into effect-intrinsic and domain-intrinsic categories. This differentiation facilitates the integration of domain-specific causal graphs into a unified joint causal graph via shared effect-intrinsic exogenous variables. We propose leveraging Neural Causal models within this joint framework to enable accurate counterfactual generation under standard identifiability assumptions. Furthermore, we introduce a novel loss function that effectively segregates effect-intrinsic from domain-intrinsic variables during model training. Given a factual observation, our framework combines the posterior distribution of effect-intrinsic variables from the source domain with the prior distribution of domain-intrinsic variables from the target domain to synthesize the desired counterfactuals, adhering to Pearl’s causal hierarchy. Intriguingly, when domain shifts are restricted to alterations in causal mechanisms without accompanying covariate shifts, our training regimen parallels the resolution of a conditional optimal transport problem. Empirical evaluations on a synthetic dataset show that our framework generates counterfactuals in the target domain that very closely resemble the ground truth.

et al., 2020) to computer vision (Pan & Bareinboim, 2024; Yang et al., 2020; De Sousa Ribeiro et al., 2023; Dash et al., 2022) and natural language processing (Jin et al., 2023; Wu et al., 2023; Hu & Li, 2021; Wang et al., 2024), etc. While some applications employ the term ”counterfactual” informally (Jeanneret et al., 2024; Lang et al., 2023), this work adopts the formal definition of structural counterfactuals as per Pearl’s hierarchy of causation (Bareinboim et al., 2022; Pearl, 2013). Current research on counterfactual inference typically confines itself to single domains or fixed causal models, neglecting potential domain shifts or alterations in causal mechanisms. Motivated by the growing interest in cross-domain learning, we address scenarios where the causal model experiences a general domain shift. Specifically, we allow both the causal graph and the underlying causal mechanisms to vary between domains, alongside possible covariate shifts (Zhang et al., 2013). For simplicity, our focus is on the two-domain case, though our framework readily extends to multiple domains. We consider an unsupervised setting where parallel or joint data across domains is unavailable. Instead, observational data and causal graphs are provided separately for each domain. This approach is more practical, as simultaneous observation of cause-effect relationships before and after a domain shift may be infeasible in practice. However, it introduces significant challenges compared to traditional counterfactual generation. To the best of our knowledge, counterfactual generation under such unsupervised domain shifts is an unexplored problem in the literature.

To adequately define structural counterfactuals, a joint causal graph that includes all cause & effect variables across both domains is required. We construct this joint graph by distinguishing cause variables into two categories: those intrinsic to the effect variable and those intrinsic to the domain. For instance, in image generation, the effect-intrinsic variable could represent the object’s identity, while the domain-intrinsic variable might denote the rendering style (e.g., cartoon versus artist-drawn images (Kim et al., 2020)). We integrate the two causal graphs by fusing their effect-intrinsic variables (both endogenous and exogenous), as illustrated in Figure 1. Here, subscripts S and T denote the source and target domains, respectively. Exogenous variables are categorized into C (effect-intrinsic) and N (domain-intrinsic),

1. Introduction

Counterfactual inference and generation are tasks that have diverse applications in a myriad of fields ranging from biology (Marchezini et al., 2022; Feuerriegel et al., 2024; Qiu

with X representing effect-intrinsic endogenous variables¹. This fusion of C, X in the joint causal graph² ensures that the effects in both domains differ solely by their domain-intrinsic variables³. Although we assume identical causal graph structures across domains for clarity of presentation, our methodology can accommodate variations in causal graph structures and interconnects between cause variables.

Consequently, we formally define our novel counterfactual generation task as follows: given a factual observation (x^s, y^s) in the source domain, generate counterfactual samples in the target domain, $Y_{x_{\text{intv}} \leftarrow x}^T | x^s, y^s$, where x_{intv} is the intervention value for x . Essentially, this involves predicting how the effect Y would appear in the target domain after intervening on the cause x to take the value x_{intv} , given the source observation (x^s, y^s) . If the causal mechanisms within the joint model are known, counterfactual inference can proceed through Pearl’s three-step process (Pearl, 2009). In practice, the causal mechanisms of the joint graph are unknown and must be learned. We propose using Neural Causal Models (NCMs) (Xia et al., 2021), which are effective for classical counterfactual generation. Training a joint NCM is challenging due to the absence of joint samples. However, since the causal mechanisms remain consistent during sampling, it suffices to learn the causal mechanisms separately for the source and target domains using domain-specific observational data. Accurate identification of exogenous variables is crucial to ensure correct counterfactual inferences. To achieve this, we introduce a novel loss term that facilitates the correct identification of effect-intrinsic variables C . Following the learning of a joint NCM, we model the posterior using a neural push-forward generator trained with a Wasserstein-based loss (Frogner et al., 2015; Arjovsky et al., 2017). The three-step counterfactual generation process is then seamlessly implemented using the learned joint NCM and posterior model.

In scenarios where domain shifts involve only changes in causal mechanisms without covariate shifts, we show that our joint model corresponds with the optimal transport (OT) plan in a conditional OT framework (Manupriya et al., 2024). This relationship extends existing works that utilize OT for sample generation under domain shifts (Korotin et al., 2023). To validate our methodology for this novel task, we crafted source and target causal mechanisms adhering to standard identifiability conditions (Nasr-Esfahany et al.,

2023; Nasr-Esfahany & Kiciman, 2023). These mechanisms were selected to allow exact computation of the exogenous posterior, thereby precisely determining the counterfactual distribution. Our simulations demonstrate that the proposed methodology correctly estimates the shifted groundtruth counterfactual via a popular two sample test (Schrab et al., 2023).

2. Background

We begin by laying out certain pre-requisites in causality theory (we borrow the notation of (Xia et al., 2021) in this regard) and kernels least squares loss that are pertinent to the contributions of this paper, followed by analyzing some prior work that is arguably most closely related to our contributions in this paper. In general we denote random variables by uppercase letters (W) and their corresponding values by lowercase letters (w). We denote by \mathcal{D}_W the domain of W and by $P(W = w)$ the probability of W taking the value w under the probability distribution $P(W)$. We denote by $\Omega(W)$ the domain of values for a random variable W . Bold font on a semantic letter indicates a set.

2.1. Preliminaries

Structural Causal Model An SCM \mathcal{M} is defined as a tuple $\langle \mathbf{U}, \mathbf{V}, \mathcal{F}, P(\mathbf{U}) \rangle$, where \mathbf{U} is a set of exogenous variables with distribution $P(\mathbf{U})$, \mathbf{V} the endogenous variables, and $\mathcal{F} \equiv \{f_1, \dots, f_n\}$ is a set of functions/mechanisms, where each $f_i : \mathbf{U}_i \times \mathbf{A}_i \rightarrow V_i, \mathbf{U}_i \subset \mathbf{U}, \mathbf{A}_i \subset \mathbf{V} \setminus \{V_i\}$. In simple words, \mathbf{V} are the observed variables, \mathbf{U} are the unobserved variables, and each mechanism (f_i) takes as input some subset of exogenous (\mathbf{U}_i) and endogenous variables (\mathbf{A}_i) and causes/outputs the corresponding observed variable (V_i). Given a *recursive* SCM, a directed graph is readily induced, in which the nodes correspond to the endogenous variables \mathbf{V} , while the directed edges correspond to the causal mechanism from each variable in \mathbf{A}_i to V_i . It is assumed that this directed graph is acyclic and as such, \mathbf{A}_i are the parents of V_i in this DAG. Every causal diagram is associated with a set of \mathcal{L}_1 constraints, which is a set of conditional independences, \mathcal{L}_2 constraints, popularly known as the do-calculus rules for interventions and finally, \mathcal{L}_3 constraints, rules that the counterfactual distributions satisfy. Every counterfactual distribution induced by the SCM satisfies all three levels of constraints. Using these 3-layered rules, various statistical, interventional, and counterfactual inferences can be performed in a systematic way. Notably, distributions in the lower levels of the causal hierarchy may not satisfy constraints of higher levels. Since in most applications the cause-effect relations are known rather than the SCM itself, one interesting modeling question is, given a causal graph, can we come up with a convenient model that is consistent with all the three levels of constraints induced

¹For simplicity, endogenous domain-intrinsic variables are assumed absent. If present, they remain separate, similar to N .

²Although such fusing of graphs is also done in twin networks (Vlontzos et al., 2021), both the causal graphs and mechanisms are assumed to be domain-invariant, whereas we allow both to vary.

³The fused effect-intrinsic variables are chosen to be same as those in the source domain, because the factual is assumed to be on the source side and the counterfactual is expected on the target side. In case of the converse, the fused variables must be chosen as those in the target domain.

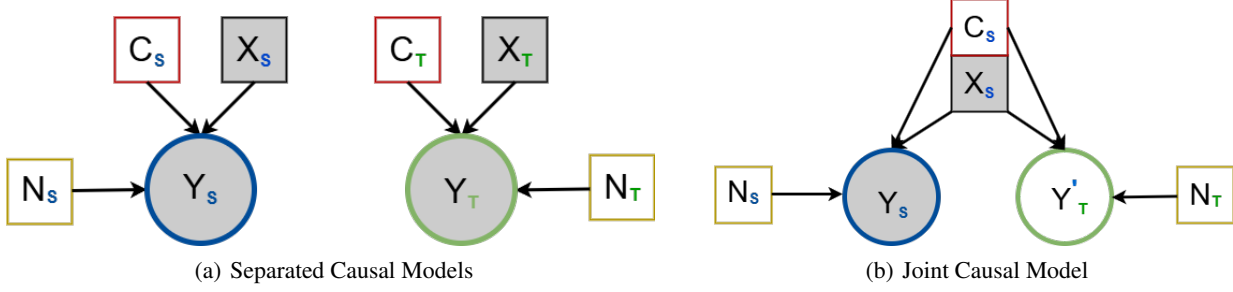


Figure 1: Illustration explaining the creation of the joint causal graph from individual graphs. Shaded nodes indicate observed variables. Y'_T differs from Y_T in the prior for C : they are abducted from the source, target domains respectively.

by the graph? NCMs are one such example of a convenient family of causal models.

Definition 2.1. NCM, Defn.2 in (Xia & Bareinboim, 2024) Given a causal diagram \mathcal{G} , a \mathcal{G} -constrained NCM $\widehat{\mathcal{M}}_\theta$ over \mathbf{V} with parameters $\theta = \{\theta_{V_i} : V_i \in \mathbf{V}\}$ is an SCM $\langle \widehat{\mathbf{U}}, \widehat{\mathbf{V}}, \widehat{\mathcal{F}}, P(\widehat{\mathbf{U}}) \rangle$ such that (1) $\widehat{\mathbf{U}} = \{\widehat{U}_C : C \in \mathcal{C}(\mathcal{G})\}$, where $\mathcal{C}(\mathcal{G})$ is the set of all maximal cliques over bi-directional edges of \mathcal{G} ; (2) $\widehat{\mathcal{F}} = \{\widehat{f}_{V_i} : V_i \in \mathbf{V}\}$, where each \widehat{f}_{V_i} is a feedforward neural net parameterized by $\theta_{V_i} \in \theta$ mapping $\mathbf{U}_{V_i} \cup \mathbf{A}_{V_i}$ to V_i for $\mathbf{U}_{V_i} = \{\widehat{U}_C \in \widehat{\mathbf{U}} : V_i \in C\}$ and $\mathbf{A}_{V_i} = A_{\mathcal{G}}(V_i)$; (3) $\text{Unif}(0, 1) \mapsto P(\widehat{U}), \forall \widehat{U} \in \widehat{\mathbf{U}}$.

Note that point 3 in Definition 2.1 above critically lies on the fact that there always exists a neural network that can transform $\text{Unif}(0, 1)$ to an arbitrary distribution P (cf. Lemma 5 in (Xia et al., 2021)). To facilitate easier learning of NCMs, we assume $\mathcal{N}(0, 1) \mapsto P(\widehat{U}), \forall \widehat{U} \in \widehat{\mathbf{U}}$ in this work. Note that Lemma 5 can be trivially extended to this case.

Kernel Least Squares It is well known that $\mathbb{E}[Y|X] = \text{argmin}_f \mathbb{E}[\|f(X) - Y\|^2]$ (Brockwell, 1991). When the kernel embeddings of Y are used instead, it is known as kernels least squares, written as: $\mathbb{E}[\Phi(Y)|X] = \text{argmin}_f \mathbb{E}[\|f(X) - \Phi(Y)\|^2]$, where Φ is the canonical feature map corresponding to a kernel. In case the kernel is characteristic (Sriperumbudur et al., 2011), $Y \mapsto \mathbb{E}[\Phi(Y)|X]$ is injective and characterizes the distribution of Y . Common examples of characteristic kernels include the radial basis function (RBF) kernel and inverse multi-quadratic kernel (IMQ) kernel among others. Thus, kernel least-squares loss is well-suited for learning conditional distributions (e.g., see (Manupriya et al., 2024) which provides empirical and theoretical results in this regard). We espouse the following derivation from (Manupriya et al., 2024), which shows how to learn a conditional generator using joint samples, without having to resort to Monte Carlo methods. Let \mathcal{D} be a given dataset of samples drawn from the joint distribution of random variables P, Q and let $\pi_{Q|P}^\gamma$ be a parametrized (by γ) conditional generator that we wish

to learn. Accordingly, we wish $\pi_{Q|P}^\gamma(\cdot|p) = s_{Q|P}(\cdot|p), \forall p \in \Omega(P)$. Utilizing the injectivity of a characteristic kernel Φ , we can equivalently rewrite the desired condition as $\int_{\Omega(P)} \left\| \mathbb{E}_{\pi_{Q|P}^\gamma(\cdot|p)}[\Phi(Y)] - \mathbb{E}_{s_{Q|P}(\cdot|p)}[\Phi(Y)] \right\|_2^2 ds_P(p) = 0$. The kernels least squares loss inside the above integral is commonly known as the squared Maximum Mean Discrepancy error, aka MMD^2 . For the rest of this paper, we take Φ to be the IMQ kernel defined as $k(x, y) = \frac{1}{\sqrt{\varrho + \|x - y\|_2^2}} \forall x, y \in \mathbb{R}^d$, where ϱ is a non-negative hyper-parameter. This is because we usually observe good results with this kernel. Next, they apply a standard result kernel mean embeddings, (Muandet et al., 2017), which states that $\mathbb{E}[\|G - h(P)\|^2] = \mathbb{E}[\|G - \mathbb{E}[G|P]\|^2] + \mathbb{E}[\|\mathbb{E}[G|P] - \mathbb{E}[h(P)]\|^2]$, when G is the kernel mean embedding of δ_Q and $h(P)$ the kernel mean embedding of $\pi_{Q|P}^\gamma(\cdot|P)$. This helps us simplify the integral over the marginal of P in terms of a marginal over the joint distribution of P, Q , since $\int_{\Omega(P)} \text{MMD}^2(\pi_{Q|P}^\gamma(\cdot|p), s_{Q|P}(\cdot|p)) ds_P(p) + \vartheta(s) = \int_{\Omega(P) \times \Omega(Q)} \text{MMD}^2(\pi_{Q|P}^\gamma(\cdot|p), \delta_Q) ds_P, Q(p, q)$, where $\vartheta(s) \geq 0$ is purely a function of the dataset and therefore, does not affect the minima of the right hand side of the equation above. The left hand side integral can be readily estimated empirically, as $\frac{1}{|\mathcal{D}|} \sum_{i=1}^{|\mathcal{D}|} \left\| \frac{1}{\kappa} \sum_{\tilde{q}_i \sim \pi_{Q|P}^\gamma(\cdot|p_i)} \Phi(\tilde{q}_i) - \Phi(q_i) \right\|^2$. Training the conditional generator over the dataset \mathcal{D} thereby is tantamount to minimizing the previously mentioned empirical estimate with respect to the parameters, γ . This "trick" is repeatedly used in most of our losses.

2.2. Prior Work

Disentanglement Despite the vast amount of literature in disentanglement particularly in the context of causal representation learning (), there are only a few that are close to the exact setting we assume in this work. (von Kügelgen et al., 2021) also studied causally disambiguating domain intrinsic exogenous variables ("style") and an effect intrinsic variables ("context"), but they assume the dataset for either

domain to be sampled using the same context distribution, whereas we allow for different observed context distributions in the observational data (cf. Figure 1). (Morioka & Hyvarinen, 2023; Daunhawer et al., 2023) extended the above work and theoretically analyzed the above setting, known as "multimodal" SCMs. However, they all seem to assume access to paired data across domains that share the same context, which we don't. Additionally, our kernel-based losses critically differ from their contrastive loss based approaches. Lastly, our setting for unpaired observed data is closest to the Out-Of-Variable generalization setting proposed in (Guo et al., 2024), but we specifically solve (counterfactual) generative tasks in this setting, whereas they restrict themselves to discriminative tasks.

Domain Shifts Informally known by various names in the literature such as Domain Adaptation (DA) ((Farahani et al., 2021; Liu et al., 2022)), Translation ((Isola et al., 2017; Lin et al., 2019)), etc. The underlying idea is to train a model using a samples from one distribution, i.e. the source, and be able to predict objects belonging to another distribution, termed as the target distribution. Whilst a plethora of such works exist in this area, to the best of our knowledge, it appears that a causal angle to this problem has largely been overlooked. (Magliacane et al., 2018) proposes a causal DAG modeling domain adaptation and incorporates a context variable, as we also do. (Teshima et al., 2020) on the other hand delves into this approach deeper and attempts to model the DA problem via structural equation models, but relies on the assumption of having the data generative mechanism to be invariant across domains. Our methodology however, admits different priors as well as mechanisms across domains. Lastly, (Zhang et al., 2015) also examine the DA problem in a simple two-variable setting and demonstrate conditions for transfer of the relevant context across domains by considering the appropriate prior and posterior distributions of the target domain. However, they constrain the causal mechanism to linear structural equations. Furthermore, none of the above works involve answering counterfactual queries in the target domain, nor deal with counterfactual generation in its rigorous form.

3. Problem Definition and Proposed Methodology

Consider the joint model presented in Figure 1. Y_S and Y_T represent the effect variables in the source and target domains respectively. Each of these is causally influenced by a common set of effect-intrinsic attributes: X (endogenous), and C (exogenous). The exogenous domain-intrinsic variables N_S and N_T are assumed to be independent of each other and need not have the same distribution. In other words, the effect variable has the same effect-intrinsic causes both before and after the domain shift. The effect

variables may hence only differ in their domain-intrinsic causes, which is meaningful. Overall, the model is assumed to be Markovian to avoid non-identifiability issues ((Nasr-Esfahany & Kiciman, 2023; Nasr-Esfahany et al., 2023)). Other such assumptions leading to identifiability are also fine. As noted earlier, the causal mechanism generating the effect variables may change with the domain shift. Thus, we denote $Y_S \equiv \mathcal{M}^{Y_S^*}(X_S, C_S, N_S)$ and $Y_T \equiv \mathcal{M}^{Y_T^*}(X_T, C_T, N_T)$, following the given source and target causal graphs. We now formally define our novel generation problem:

Problem 3.1 (Counterfactual Translation). *Let (x, y) be a given sample from the joint distribution $\mathcal{P}(X_S, Y_S)$ induced by the source causal mechanism $\mathcal{M}^{Y_S^*}(\cdot, \cdot, \cdot)$. Let $C_{S|(x,y)}$ denote a random variable obeying the posterior distribution induced over C_S , by conditioning on (x, y) in the source mechanism $\mathcal{M}^{Y_S^*}(\cdot, \cdot, \cdot)$. Given a value x_{inv} , the task is to generate samples corresponding to the distribution induced by $\mathcal{M}^{Y_T^*}(x_{inv}, C_{S|(x,y)}, N_T)$.*

To motivate this problem, consider the task of person re-identification in surveillance systems, which is crucial for tracking individuals across different camera views in public spaces such as airports or train stations ((Ye et al., 2022)). For the sake of this illustration, we extend this to a case where a suspect needs to be tracked for migration between tourist locations of two different countries with starkly clothing traditions. Imagine that we have two sets of images: one from images of people in region S and the other from those in region D , each of them with their native attires respectively. These images may not overlap, and we do not have paired samples showing the same individual captured in both locations. The task is to generate highly probable images of the suspect in the clothing style native to region D , given the information that the suspect has blended themselves with the local clothing culture. Furthermore, due to the passage of time and local weather conditions in region D , we may assume that certain attributes such as the age, skin color, etc. have changed, that are also provided as additional information. Incorporating this additional information is however, non-trivial. With no paired training data linking the source and target images, one needs to generate a plausible counterfactual version of the person in the source image, conditioned on images representing the person in region S , along with interventions indicating a change in appearance such as age or skin color, and then translate this counterfactual image to the style of clothing adopted in region D .

We can now elucidate correspondences of different variables of interest in the formal definition of the problem described above to that setting. X_S models intervenable attributes such as 'age', 'skin color', etc. and obeys the distribution of such attributes as observed in region S . Analogously, X_T models the same in region T . While the attributes se-

manically allude to the same concepts, the distributions of these variables can differ significantly across regions due to varied reasons such as geography, climate, local culture, etc. C_S models latent variables that roughly capture the identity of the person, such as their silhouette, posture, etc. These are not explicitly annotated for in the dataset, yet need to be captured to produce an accurate counterfactually translated image of the suspect. Thus conditioning on the known age/skin color of the person and their image in region S would tantamount to inducing a posterior distribution of silhouettes/postures particularly identifying the suspect. Finally, the domain-intrinsic exogenous variables N_S, N_T may capture other unobserved variables such as the clothing culture in the respective regions etc.

3.1. Modeling and Training

We propose modeling causal mechanisms of interest using NCMs, because of their versatility and competence in executing counterfactually generative tasks (Xia et al., 2023). We model the true source and target causal mechanisms $\mathcal{M}^{Y_S^*}, \mathcal{M}^{Y_T^*}$ using neural networks $\widehat{\mathcal{M}}_{\theta_S}^{Y_S}, \widehat{\mathcal{M}}_{\theta_T}^{Y_T}$ with parameters θ_S, θ_T respectively. However, we lack explicit supervision for the exogenous variables, $C_{S/T}, N_{S/T}$. Therefore, we adopt a trick promulgated by (Xia et al., 2021), wherein we technically model wherein $\widehat{\mathcal{M}}_{\theta_S}^{Y_S}, \widehat{\mathcal{M}}_{\theta_T}^{Y_T}$ attempt to align with the equivalent (groundtruth) causal models $\widehat{\mathcal{M}}^{Y_S^*}, \widehat{\mathcal{M}}^{Y_T^*}$, where $\widehat{C}_{S/T}, \widehat{N}_{S/T} \sim \mathcal{N}(0, \mathbb{I}_{d \times d})$.

Furthermore, we propose modeling the exogenous variables $C_{S/T}, N_{S/T}$, using push-forward neural generators, that conjoined with $\widehat{\mathcal{M}}_{\theta_S}^{Y_S}, \widehat{\mathcal{M}}_{\theta_T}^{Y_T}$, would mimic the structural effect of the exogenous variables on the output causal variables $Y_{S/T}$. Specifically, let $C_S \equiv m_{\phi_{C_S}}^{C_S \#}(\eta^{C_S}), C_T \equiv m_{\phi_{C_T}}^{C_T \#}(\eta^{C_T})$, where η^{C_S}, η^{C_T} are samples from a noise distribution that is easy to sample from, e.g. Gaussian. Similarly, let $N_S \equiv m_{\zeta_{N_S}}^{N_S \#}(\eta^{N_S}), N_T \equiv m_{\zeta_{N_T}}^{N_T \#}(\eta^{N_T})$. Note that such careful modeling of the exogenous variables is needed for two reasons: (i) we wish to disambiguate between the effect-intrinsic and domain-intrinsic variables (ii) the distribution of C_S need not be same as that of C_T . Similarly, the distribution of N_S need not be same as that of N_T . Classical counterfactual models need not resort to such careful modeling and can safely assume $m_{\phi_{C_{S/T}}}^{C_{S/T} \#}(\eta^{C_{S/T}}), m_{\zeta_{N_{S/T}}}^{N_{S/T} \#}(\eta^{N_{S/T}})$ are some hidden sub-networks in $\widehat{\mathcal{M}}_{\theta_S}^{Y_S}, \widehat{\mathcal{M}}_{\theta_T}^{Y_T}$ itself.

The main reason why training the described joint model is challenging is because it is not practical to assume that the joint samples are available. As mentioned earlier, we make a more practical assumption that cause-effect samples from the source and target models are separately available. Consequently, let $(x_1^S, y_1^S), \dots, (x_{m_1}^S, y_{m_1}^S)$ de-

note the observational data in the source domain and let $(x_1^T, y_1^T), \dots, (x_{m_2}^T, y_{m_2}^T)$ denote the observational data in the target domain. Our losses significantly differ from (Xia et al., 2021) in that we mostly train our models via a kernels least squares loss between samples of appropriate distributions whereas they train using negative log-likelihood. Since the causal mechanisms are independent of the sampling procedure, the mechanisms for generating Y_S, Y_T in the source, target-specific NCMs and in the joint NCM are the same. Hence, the source and target observational data can be used to train the networks in the joint model to be \mathcal{L}_1 consistent with the true mechanisms. For instance, on the source side the goal is to learn $\widehat{\mathcal{M}}_{\theta_S}^{Y_S}(X_S, \cdot, \cdot)$ such that $P_{\widehat{\mathcal{M}}_{\theta_S}^{Y_S}}(X_S, \cdot, \cdot) = P_{\widehat{\mathcal{M}}_{\theta_S}^{Y_S^*}}(X_S, \cdot, \cdot)$. To this end, we critically employ the fact that any characteristic kernel Φ induces an injective map over distributions, stated in Section 2.1, as follows:

$$\begin{aligned} P_{\widehat{\mathcal{M}}_{\theta_S}^{Y_S}}(X_S, \cdot, \cdot) &= P_{\widehat{\mathcal{M}}^{Y_S^*}}(X_S, \cdot, \cdot) \Leftrightarrow P_{\widehat{\mathcal{M}}_{\theta_S}^{Y_S}}(X_S = x, \cdot, \cdot) \\ &= P_{\widehat{\mathcal{M}}^{Y_S^*}}(X_S = x, \cdot, \cdot), \forall x \in \Omega(X_S) \Leftrightarrow \forall x \in \Omega(X_S), \\ \mathbb{E}_{Y_S \sim P_{\widehat{\mathcal{M}}_{\theta_S}^{Y_S}}(X_S = x, \cdot, \cdot)}[\Phi(Y_S)] &= \mathbb{E}_{Y_S \sim P_{\widehat{\mathcal{M}}^{Y_S^*}}(X_S = x, \cdot, \cdot)}[\Phi(Y_S)]. \end{aligned} \quad (1)$$

Consequently, we aim to learn a conditional generator $\widehat{\mathcal{M}}_{\theta_S}^{Y_S}$, using joint samples $\{(x_i^S, y_i^S)\}_{i=1}^n$. This is our preferred loss to train over observational data due to its demonstrated superior performance compared to other traditional losses such as adversarial/KL/Wasserstein losses (Manupriya et al., 2024). In particular, we use the MMD² loss between the sample kernel means of the conditional distributions $P_{\widehat{\mathcal{M}}_{\theta_S}^{Y_S}}(\widehat{C}_S, \widehat{N}_S | X_S = x)$ and $P_{\widehat{\mathcal{M}}^{Y_S^*}}(\widehat{C}_S, \widehat{N}_S | X_S = x)$ as follows:

$$\begin{aligned} \ell_{\text{gen}}^S(\theta_S, \phi_{C_S}, \zeta_{N_S}) &= \frac{1}{n_{\text{gen}}^S} \sum_{i=1}^{n_{\text{gen}}^S} \left\| \Phi(y_i^S) - \right. \\ &\left. \frac{1}{q_{\text{gen}}^S} \sum_{j=1}^{q_{\text{gen}}^S} \Phi \left(\widehat{\mathcal{M}}_{\theta_S}^{Y_S} \left(x_i^S, m_{\phi_{C_S}}^{C_S \#}(\eta_{ij}^{C_S}), m_{\zeta_{N_S}}^{N_S \#}(\eta_{ij}^{N_S}) \right) \right) \right\|_{\mathcal{H}}^2. \end{aligned} \quad (2)$$

Here, n_{gen}^S is the number of samples within the training set (or within a mini-batch, if using an optimization algorithm such as mini-batch SGD) and q_{gen}^S the number of noise samples $\eta_{ij}^{C_S/N_S}$ sampled from $\mathcal{N}(0, I_{d \times d})$ per data point (x_i^S, y_i^S) , used to empirically approximate the kernel mean of Y_S when in turn sampled from $P_{\widehat{\mathcal{M}}_{\theta_S}^{Y_S}}(\widehat{C}_S, \widehat{N}_S | X_S = x)$. For the sake of completeness, we also note that alternatives from conditional generative adversarial networks based literature may also be viable to learn this conditional generator, as we do not claim the above loss as a novel contribution of our work. A similar loss is also introduced to train the target

mechanisms as shown below:

$$\ell_{\text{gen}}^T(\theta_T, \phi_{C_T}, \zeta_{N_T}) = \frac{1}{n_{\text{gen}}^T} \sum_{i=1}^{n_{\text{gen}}^T} \left\| \Phi(y_i^T) - \frac{1}{q_{\text{gen}}^T} \sum_{j=1}^{q_{\text{gen}}^T} \Phi \left(\widehat{\mathcal{M}}_{\theta_T}^{Y_T} \left(x_i^T, \widehat{m}_{\phi_{C_T}}^{C_T\#}(\eta_{ij}^{C_T}), \widehat{m}_{\zeta_{N_T}}^{N_T\#}(\eta_{ij}^{N_T}) \right) \right) \right\|_2^2. \quad (3)$$

We now make an important observation: although $\widehat{\mathcal{M}}_{\theta_T}^{Y_T}$ is trained using target domain data, when it is employed in the joint model, the distribution of its inputs is according to the source domain. This is a classical problem of covariate shift and can be easily tackled using state-of-the-art techniques that account for this shift ((FAtlas et al., 2021; Nguyen et al., 2022; Manupriya et al., 2024)). The essential idea in such methods is to solve an OT problem between the domains and employ the obtained weights while computing the least square loss. This is typically written as a corrective loss term, $\ell_{\text{CS}}(\theta_T, \phi_T, \phi_S, \zeta_T)$ (e.g., objective (6) in ((Damodaran et al., 2018))). Thus, the overall loss for training the mechanisms on the target side is $\overline{\ell}_{\text{gen}}^T(\theta_T, \phi_T, \phi_S, \zeta_T) \equiv \ell_{\text{gen}}^T(\theta_T, \phi_T, \zeta_T) + \ell_{\text{CS}}(\theta_T, \phi_T, \phi_S, \zeta_T)$.

Finally, the effect-intrinsic, domain-intrinsic variables, C, N , need to be disambiguated correctly. This cannot be done if the training of the networks happen separately using the corresponding losses. For example, if identities of C, N are interchanged, the domain-specific networks still remain the same, with an appropriate permutation of input variables. However, counterfactual inference may catastrophically fail if C, N are interchanged. Hence, we propose to jointly train the NCMs with an additional loss term that helps disambiguate the variables. To this end, we assume a cost function, dis , is available that can perceive effect-intrinsic differences in the variables and ignores the domain-intrinsic differences. For example, in the case of image generation, the cost can be taken as the L_{pips} loss (Zhang et al., 2018) or as squared Euclidean distance computed with image embeddings from a pre-trained network like AlexNet (Krizhevsky et al., 2012), VGG (Simonyan & Zisserman, 2015), Swin-T (Liu et al., 2021), etc. Such a cost will be high if, say the identity of the object depicted in the images is not the same, and low even if, say the style of rendering of the images is different and vice-versa. Our novel loss term (ℓ_{tr}) for disambiguating the variables is:

$$\sum_{i=1}^{n_{\text{tr}}} \sum_{j=1}^{q_{\text{tr}}} \text{dis} \left(\widehat{\mathcal{M}}_{\theta_S}^{Y_S} \left(x_i^S, \widehat{m}_{\phi_{C_S}}^{C_S\#}(\eta_{ij}^{C_S}), \widehat{m}_{\zeta_{N_S}}^{N_S\#}(\eta_{ij}^{N_S}) \right), \widehat{\mathcal{M}}_{\theta_T}^{Y_T} \left(x_i^S, \widehat{m}_{\phi_{C_S}}^{C_S\#}(\eta_{ij}^{C_S}), \widehat{m}_{\zeta_{N_T}}^{N_T\#}(\eta_{ij}^{N_T}) \right) \right) = \ell_{\text{tr}} \cdot (nq)_{\text{tr}} \quad (4)$$

Note that the effect-intrinsic variables are the same in the

above in both the mechanisms, whereas the domain-intrinsic variables are different. Hence, for the correct C, N pairs, this term will be low and vice-versa. In particular, if C, N are interchanged, then this term will be high. Thus, this acts as a loss function to correctly disambiguate the exogenous variables.

3.2. Inference

Given the learned joint NCM, counterfactual generation can be done using the standard three-step procedure: abduction, action, prediction. For the abduction step, we need samples from the posterior $p(c^S | x^S, y^S)$, where (x^S, y^S) is the cause-effect pair observed in the source domain. To this end, we propose modeling the posterior, $p(c^S, n^S | x^S, y^S)$, using a pushforward neural network generator, $g_\psi(x^S, y^S, N^\#)^4$. From the Bayes rule, we have: $p(c^S, n^S | x^S, y^S) p(x^S, y^S) = p(x^S) p(c^S) p(n^S) p(y^S | x^S, c^S, n^S)$, where the LHS is the factorization corresponding to the source causal graph and the RHS is the factorization involving the posterior to be estimated. Let $\mathcal{S}_{\theta_S, \phi_S, \zeta_S} \equiv \left(\Upsilon, \widehat{\mathcal{M}}_{\theta_S}^{Y_S}(\Upsilon) \right)$, be a set of samples from the source NCM, where $\Upsilon \equiv \left(x_i^S, \widehat{m}_{\phi_{C_S}}^{C_S\#}(\eta_{ij}^{C_S}), \widehat{m}_{\zeta_{N_S}}^{N_S\#}(\eta_{ij}^{N_S}) \right)$ and $\eta_{ij}^{(C/N)_S}$ are independent samples of $\mathcal{N}(0, \mathbb{I}_{d \times d})$. Let $\mathcal{P}_{\zeta_{N_S}, \psi} \equiv \left(x_i^S, g_\psi(x_i^S, y_i^S, \eta_{ij}^\#), \widehat{m}_{\zeta_{N_S}}^{N_S\#}(\eta_{ij}^{N_S}), y_i^S \right)$, i.e. samples from the posterior, where $\eta_{ij}^{N_S}, \eta_{ij}^\#$ are independent samples from $\mathcal{N}(0, \mathbb{I}_{d \times d})$. With this notation, the loss for training g_ψ turns out to be:

$$\ell_{\text{pos}}(\theta_S, \phi_S, \zeta_S, \psi) \equiv \mathbb{W}(\mathcal{S}_{\theta_S, \phi_S, \zeta_S}, \mathcal{P}_{\zeta_{N_S}, \psi}), \quad (5)$$

where, \mathbb{W} is an appropriate distance between between measures like the Wasserstein metric ((Frogner et al., 2015)). The training of the inference network can either be done jointly with the NCMs, in which case the optimization problem is:

$$\min_{\theta_S, \phi_S, \zeta_S, \theta_T, \phi_T, \zeta_T, \psi} \ell_{\text{gen}}^S + \overline{\ell}_{\text{gen}}^T + \ell_{\text{tr}} + \ell_{\text{pos}} \quad (6)$$

or, can be trained separately in which case the optimization problems are:

$$\begin{aligned} (\theta_S^*, \phi_S^*, \zeta_S^*, \theta_T^*, \phi_T^*, \zeta_T^*) &\equiv \text{argmin} \ell_{\text{gen}}^S + \overline{\ell}_{\text{gen}}^T + \ell_{\text{tr}}, \quad (7) \\ \psi^* &\equiv \text{argmin}_\psi \ell_{\text{pos}}(\theta_S^*, \phi_S^*, \zeta_S^*, \psi) \end{aligned}$$

Once the optimal network parameters are obtained by solving the appropriate optimization problems using solvers like AdamW, counterfactual samples in the target domain can be produced by:

⁴ $N^\#$ is the pushforward noise.

1. Sampling from posterior using $g_{\psi_*}(x_s, y_s, N^\#)$. Different $n^\#$ samples from the reference Gaussian will produce different samples from the posterior.
2. Counterfactual samples are obtained using $\widehat{\mathcal{M}}_{\theta_s^*}^{Y_T} \left(x_{\text{intv}}, g_{\psi} \left(x^S, y^S, \eta_{ij}^\# \right), \widehat{m}_{\zeta_{N_T}^\#} \left(\eta_{ij}^{N_T} \right) \right)$. Different $\eta^\# / N_T \sim \mathcal{N}(0, I_{d \times d})$ samples produce different samples from the counterfactual distribution.

3.3. Connection to Conditional Optimal Transport

Interestingly, in the special case where the distributions of the exogenous variables are the same in the source and the target domains⁵, (7) can be interpreted as a conditional OT problem. Let $p_{\theta_s, \phi_s}(y^S | x^S, \eta^{C_s}), p_{\theta_T, \phi_s}(y^S | x^S, \eta^{C_s})$ denote the distributions induced by the left & right arguments to dist in (7) respectively. Furthermore, let $p_{\phi_s}(\eta)$ denote the distribution induced by $\widehat{m}_{\phi_{C_s}^\#}$. Let $p_S(x^S)$ denote the distribution of X_S . With this notation, it is easy to see that ℓ_{tr} is the sample mean corresponding to:

$$\int p_{\theta_s, \phi_s}(y^S | x^S, \eta^{C_s}) p_{\theta_T, \phi_s}(y^S | x^S, \eta^{C_s}) d(y^S, y^T) \quad (8)$$

$$\int \int \Theta(x^S, \eta^{C_s}) p_{\phi_s}(\eta) p_S(x^S) d(n^{C_s}, x^S)$$

$$= \mathbb{E}_{X_S, C_S} \left[\mathbb{E} \left[d(Y_S, Y_T) | X_S, C_S \right] \right],$$

where the total expectation is w.r.t. the joint causal model being learned⁶. Also, the source side marginal of this joint conditioned on x^S is given by $\int p_{\theta_s, \phi_s}(y^S | x^S, \eta) p_{\phi_s}(\eta) d\eta$. The kernel least squares term in ℓ_{gen}^S matches this marginal to the distribution of $Y_S | x^S$ in the source dataset. Likewise, the ℓ_{gen}^T can be understood as a term for matching the target side conditional to $Y_T | x^S$. Moreover, if the distributions of the exogenous variables are the same, there is no covariate shift and hence ℓ_{gen}^T is same as ℓ_{gen}^T in (7). In such a case, (7) becomes same as (6) in (Manupriya et al., 2024) (apart from the parametrization of the transport plan) and hence can be interpreted as a conditional OT problem between $p(y^S | x^S)$ and $p(y^T | x^S)$. Thus this connection seems to generalize the idea of employing OT based methods for applications like image-to-image translation (Korotin et al., 2023), which is an example of generative modeling under domain shift (without any reference to causality). To summarize, in the special case where the domain shift is purely a conditional shift (change in causal mechanism) without any covariate shift, our model learned is essentially an OT plan corresponding to the conditional OT problem between $p(y^S | x^S)$ and $p(y^T | x^S)$. Nevertheless, even in this special case, our parametrization of the transport plan (joint) in terms of the effect-intrinsic variable C_S is crucial for counterfactual generation.

⁵ $C_S \sim C_T, N_S \sim N_T$.

⁶ $\Theta(x^S, \eta^{C_s})$ is the first integral.

4. Simulations

We present the details of the synthetic dataset on which we test our methodology. Due to the lack of an existing baseline tailored for this novel task, we introduce the following benchmark dataset that obeys the causal graph depicted in Figure 1, with structural equations that are described below.

4.1. Dataset

The SCMs of the source and target domains consist of X, C, N variables that are of dimension $d \times 1$. The corresponding effect variables in both domains i.e., Y are of dimension $2d \times 1$, while their structural equations read as:

$$Y_S = \left[\begin{array}{c} \mathcal{A}_S e^{C_S} / 2 \\ (C_S \odot N_S) + X_S \end{array} \right], \quad (9)$$

$$Y_T = \left[\begin{array}{c} (C_T \odot N_T^2) + X_T \\ \mathcal{A}_T e^{C_T} \end{array} \right], \quad (10)$$

where $\mathcal{A}_{S/T} = \mathcal{B}^T \mathcal{B} + 5I_{d \times d}$, and $\mathcal{B}_{S/T} = X_{S/T} (2^{X_{S/T}})^T$. In this context, the symbol \odot denotes a Hadamard product, and 'T' in the superscript refers to the transpose operation over a tensor. Likewise, the notation of the form a^X, X^b for $a, b \in \mathbb{R}$ denote exponentiation to the base a , raising to the power of b for each individual element of the vector $X \in \mathbb{R}^d$, respectively. The priors for the causal variables of the source & target domains are:

$$X_S \sim \text{Uniform}(-1, 1), \quad \widetilde{X}_T \sim \text{ContinuousBernoulli}(0.6),$$

$$\widetilde{C}_S \sim \text{Beta}(4, 5), \quad C_T \sim \text{Normal}(0, I_{d \times d}),$$

$$N_S \sim \text{vonMises}(0, 4), \quad N_T \sim \text{Normal}(0, 0.1 \cdot I_{d \times d}). \quad (11)$$

In fact, we pick C_S, X_T to be an affine transforms of $\widetilde{C}_S, \widetilde{X}_T$ respectively, as $C_S = 1_{d \times 1} - (2 \cdot \widetilde{C}_S)$, $X_T = 1_{d \times 1} - (2 \cdot \widetilde{X}_T)$. For the target domain, we explicitly choose different priors so as to establish a strong benchmark that does not utilize spurious correlations across variables and domains.

4.1.1. COMPUTING SHIFTED COUNTERFACTUALS

A key property of the proposed dataset is that the source-side mechanism is invertible, given the values of X_S, Y_S . This is in line with invertibility assumptions often made in the SCM community (Nasr-Esfahany et al., 2023; Poinot et al., 2024). Let $Y_S[:d], Y_S[d:]$ denote the first and last d elements of $Y_S \in \mathbb{R}^{2d}$ respectively. Then, given X_S, Y_S , we can compute $C_S = \mathcal{A}_S^{-1} Y_S[:d]$. Notice that by design, $\mathcal{A}_{S/T}$ is always positive definite and hence invertible, so such an inverse is always defined. Using this C_S we can then compute $N_S = (Y_S[d:] - X_S) / C_S$. Thus for each triplet $(x_{\text{intv}}, x_{\text{fact}}, y_{\text{fact}})$, there exists a unique counterfactual for that in the source domain. However, this

is not the case in the target domain. Though C_T is exactly retrievable given X_T, Y_T, N_T is not, since there are at least two solutions for it given X_T, Y_T and C_T , namely $N_T = \pm \sqrt{(Y_T[d:] - X_T)/C_T}$. This illustrates that the distribution of shifted counterfactuals is crucially dependent on the target side mechanism. Thus, to generate shifted counterfactual groundtruth samples, we follow the procedure outlined below:

1. Sample x_{intv}^T for the target domain from any distribution with identical support as the prior of X_T . For simplicity, we may choose this distribution to be the prior of X_T itself.
2. Sample $x_{\text{fact}}^S, c^S, n^S$ from the priors of X_S, C_S, N_S respectively. Generate the corresponding y_{fact}^S using Equation 9. Accordingly we randomly select a pair $(x_{\text{fact}}^S, y_{\text{fact}}^S)$.
3. Using the invertibility of Equation 9, compute c_{fact}^S for the chosen $(x_{\text{fact}}^S, y_{\text{fact}}^S)$ pair.
4. Sample n^T from the prior of N_T and then plug $x_{\text{intv}}^T, c_{\text{fact}}^S, n^T$ into Equation 10 to generate samples from the distribution of shifted counterfactuals.

The distribution of shifted counterfactuals considered above is as conditioned on a particular triplet $(x_{\text{intv}}^T, x_{\text{fact}}^S, y_{\text{fact}}^S)$. Sampling multiple such triplets and generating corresponding shifted counterfactuals then corresponds to generating joint samples of shifted counterfactuals paired with their causal variables of interest.

4.2. Results

We test our proposed methodology on the above specified dataset with $d = 1$, as this is sufficient to demonstrate the generation of shifted counterfactuals. When training on this dataset as per Equation 6, we simply instantiate the following MSE loss for ℓ_{tr} (cf. Equation 4):

$$\frac{1}{mq} \sum_{i=1}^m \sum_{j=1}^q \left\| \widehat{\mathcal{M}}_{\theta_S}^{Y_S}(\cdot, \phi_S, \zeta_S)[0] - \frac{1}{2} \widehat{\mathcal{M}}_{\theta_T}^{Y_S}(\cdot, \phi_S, \zeta_T)[1] \right\|_2^2. \quad (12)$$

This choice nicely fits in with the intention of disambiguating the latent context from the noise across domains. To see this, notice that the synthetic dataset proposed above bears the property that if $X_S = X_T$ and $C_S = C_T$, then $Y_S = \frac{Y_T}{2}$; thus $C_{S/T}$ satisfies an invariant across domains which $N_{S/T}$ does NOT satisfy, which in turn helps disentangle the role of C_S when performing shifted counterfactual inference.

To evaluate the quality of our shifted counterfactuals, we run a two sample test (Schrab et al., 2023) between samples from the estimated joint distribution of factu-als and shifted counterfactuals, and the

corresponding groundtruth distribution. In particular, given a pair $(x_i^S, x_{\text{intv}_i})$, we randomly sample 100 triplets $\left(\widehat{m}_{\phi_{C_S}^{\#}}^{C_S}(\eta_{ij}^{C_S}), \widehat{m}_{\zeta_{N_S}^{\#}}^{N_S}(\eta_{ij}^{N_S}), \widehat{m}_{\zeta_{N_T}^{\#}}^{N_T}(\eta_{ij}^{N_T}) \right)$ and compare samples from $\left[\widehat{y}_{ij}^S; \widehat{\mathcal{M}}_{\theta_T}^{Y_T}(x_{\text{intv}_i}, g_{\psi}(x_i^S, \widehat{y}_{ij}^S, \eta_{ij}^{\#}), \widehat{m}_{\zeta_{N_T}^{\#}}^{N_T}(\eta_{ij}^{N_T})) \right]$ and $\left[\widehat{y}_{ij}^S; \mathcal{M}^{Y_T^*}(x_{\text{intv}_i}, c_{S|(x_i^S, y_{ij}^S)}, N_T) \right]$. Here $\widehat{y}_{ij}^S / \widehat{y}_{ij}^S$ are sampled by plugging in x_i^S in the estimated /groundtruth equations and varying the context and noise from the source domain appropriately. Finally, we average the Agg-MMD two-sample test scores between samples of these distributions over 500 pairs of $(x_i^S, x_{\text{intv}_i})$ and got a 70% score with 95% confidence, proving the efficacy of our approach⁷.

We adopt the two-stage training process as explained in Equations 7. This is done to ensure that the posterior network learns to be consistent with the distribution of samples induced from the trained generator network. The hyperparameters for controlling individual loss terms are to be picked via cross-validation. Details on the architectures of the generator, context and noise networks are provided in the Appendix A.1.

5. Summary and Conclusions

In this work, we introduced the novel task of structural-counterfactual generation under general domain-shift and studied it in the practical setting where no parallel/joint data is available. It turned out that modeling and training are considerably more challenging than in classical counterfactual generation tasks. In terms of modeling, the crucial step was to separately model the effect-intrinsic and domain-intrinsic variables, so that the structural-counterfactual is well-defined. In terms of training, disambiguating the effect-intrinsic and domain-intrinsic exogenous variables to correctly learn their distributions was the challenging step. From the trained model, the procedure for sampling counterfactuals in the target domain was presented. Connections to the optimal transport problem provided more insight into the proposed methodology.

In future, we would like to explore vision, biology applications of the novel task studied in this paper. Using the connections to OT and corresponding barycenter problems, we plan to extend structural-counterfactual generation to settings of domain interpolation.

Impact Statement

This paper presents work whose goal is to advance the field of Machine Learning. There are many potential societal

⁷We will provide code upon acceptance.

consequences of our work, none which we feel must be specifically highlighted here.

References

- Arjovsky, M., Chintala, S., and Bottou, L. Wasserstein generative adversarial networks. In Precup, D. and Teh, Y. W. (eds.), *Proceedings of the 34th International Conference on Machine Learning*, volume 70 of *Proceedings of Machine Learning Research*, pp. 214–223. PMLR, 06–11 Aug 2017. URL <https://proceedings.mlr.press/v70/arjovsky17a.html>.
- Bareinboim, E., Correa, J. D., Ibeling, D., and Icard, T. *On Pearl’s Hierarchy and the Foundations of Causal Inference*, pp. 507–556. Association for Computing Machinery, New York, NY, USA, 1 edition, 2022. ISBN 9781450395861. URL <https://doi.org/10.1145/3501714.3501743>.
- Brockwell, P. J. *Time series: Theory and methods*. Springer-Verlag, 1991.
- Damodaran, B. B., Kellenberger, B., Flamary, R., Tuia, D., and Courty, N. Deepjdot: Deep joint distribution optimal transport for unsupervised domain adaptation. In *Computer Vision – ECCV 2018: 15th European Conference, Munich, Germany, September 8-14, 2018, Proceedings, Part IV*, pp. 467–483, Berlin, Heidelberg, 2018. Springer-Verlag. ISBN 978-3-030-01224-3. doi: 10.1007/978-3-030-01225-0_28. URL https://doi.org/10.1007/978-3-030-01225-0_28.
- Dash, S., Balasubramanian, V. N., and Sharma, A. Evaluating and Mitigating Bias in Image Classifiers: A Causal Perspective Using Counterfactuals . In *2022 IEEE/CVF Winter Conference on Applications of Computer Vision (WACV)*, pp. 3879–3888, Los Alamitos, CA, USA, January 2022. IEEE Computer Society. doi: 10.1109/WACV51458.2022.00393. URL <https://doi.ieeecomputersociety.org/10.1109/WACV51458.2022.00393>.
- Daunhawer, I., Bizeul, A., Palumbo, E., Marx, A., and Vogt, J. E. Identifiability results for multimodal contrastive learning. In *The Eleventh International Conference on Learning Representations*, 2023. URL https://openreview.net/forum?id=U_2kuqoTcB.
- De Sousa Ribeiro, F., Xia, T., Monteiro, M., Pawlowski, N., and Glocker, B. High fidelity image counterfactuals with probabilistic causal models. In Krause, A., Brunskill, E., Cho, K., Engelhardt, B., Sabato, S., and Scarlett, J. (eds.), *Proceedings of the 40th International Conference on Machine Learning*, volume 202 of *Proceedings of Machine Learning Research*, pp. 7390–7425. PMLR, 23–29 Jul 2023. URL <https://proceedings.mlr.press/v202/de-sousa-ribeiro23a.html>.
- Farahani, A., Voghoei, S., Rasheed, K., and Arabnia, H. R. A brief review of domain adaptation. In Stahlbock, R., Weiss, G. M., Abou-Nasr, M., Yang, C.-Y., Arabnia, H. R., and Deligiannidis, L. (eds.), *Advances in Data Science and Information Engineering*, pp. 877–894, Cham, 2021. Springer International Publishing. ISBN 978-3-030-71704-9.
- Fatras, K., Séjourné, T., Courty, N., and Flamary, R. Unbalanced minibatch optimal transport; applications to domain adaptation. In *Proceedings of the 38th International Conference on Machine Learning*, 2021.
- Feuerriegel, S., Frauen, D., Melnychuk, V., Schweisthal, J., Hess, K., Curth, A., Bauer, S., Kilbertus, N., Kohane, I. S., and van der Schaar, M. Causal machine learning for predicting treatment outcomes. *Nature Medicine*, 30(4): 958–968, April 2024. ISSN 1546-170X. doi: 10.1038/s41591-024-02902-1. URL <http://dx.doi.org/10.1038/s41591-024-02902-1>.
- Frogner, C., Zhang, C., Mobahi, H., Araya, M., and Poggio, T. A. Learning with a wasserstein loss. In Cortes, C., Lawrence, N., Lee, D., Sugiyama, M., and Garnett, R. (eds.), *Advances in Neural Information Processing Systems*, volume 28. Curran Associates, Inc., 2015. URL https://proceedings.neurips.cc/paper_files/paper/2015/file/a9eb812238f753132652ae09963a05e9-Paper.pdf.
- Guo, S., Wildberger, J. B., and Schölkopf, B. Out-of-variable generalisation for discriminative models. In *The Twelfth International Conference on Learning Representations*, 2024. URL <https://openreview.net/forum?id=zwMfg9PfPs>.
- He, K., Zhang, X., Ren, S., and Sun, J. Delving deep into rectifiers: Surpassing human-level performance on imagenet classification. In *2015 IEEE International Conference on Computer Vision (ICCV)*, pp. 1026–1034, 2015. doi: 10.1109/ICCV.2015.123.
- Hu, Z. and Li, L. E. A causal lens for controllable text generation. In Beygelzimer, A., Dauphin, Y., Liang, P., and Vaughan, J. W. (eds.), *Advances in Neural Information Processing Systems*, 2021. URL <https://openreview.net/forum?id=kAm9By0R5ME>.
- Isola, P., Zhu, J.-Y., Zhou, T., and Efros, A. A. Image-to-image translation with conditional adversarial networks. In *2017 IEEE Conference on Computer Vision and Pattern Recognition (CVPR)*, pp. 5967–5976, 2017. doi: 10.1109/CVPR.2017.632.

- Jeanneret, G., Simon, L., and Jurie, F. Text-to-image models for counterfactual explanations: a black-box approach. In *Proceedings of the IEEE/CVF Winter Conference on Applications of Computer Vision*, pp. 4757–4767, 2024.
- Jin, Z., Chen, Y., Leeb, F., Gresele, L., Kamal, O., LYU, Z., Blin, K., Adauto, F. G., Kleiman-Weiner, M., Sachan, M., and Schölkopf, B. CLadder: A benchmark to assess causal reasoning capabilities of language models. In *Thirty-seventh Conference on Neural Information Processing Systems*, 2023. URL <https://openreview.net/forum?id=e2wtjx0Yqu>.
- Kim, J., Kim, M., Kang, H., and Lee, K. H. U-gat-it: Unsupervised generative attentional networks with adaptive layer-instance normalization for image-to-image translation. In *International Conference on Learning Representations*, 2020. URL <https://openreview.net/forum?id=BJlZ5ySKPH>.
- Korotin, A., Selikhanovych, D., and Burnaev, E. Neural optimal transport. In *The Eleventh International Conference on Learning Representations*, 2023. URL <https://openreview.net/forum?id=d8CBRLWNkqH>.
- Krizhevsky, A., Sutskever, I., and Hinton, G. E. ImageNet classification with deep convolutional neural networks. In Pereira, F., Burges, C., Bottou, L., and Weinberger, K. (eds.), *Advances in Neural Information Processing Systems*, volume 25. Curran Associates, Inc., 2012. URL https://proceedings.neurips.cc/paper_files/paper/2012/file/c399862d3b9d6b76c8436e924a68c45b-Paper.pdf.
- Lang, O., Traynis, I., and Liu, Y. Explaining counterfactual images. *Nature Biomedical Engineering*, 2023. URL <https://rdcu.be/dwVKK>.
- Lin, Y.-J., Wu, P.-W., Chang, C.-H., Chang, E., and Liao, S.-W. Relgan: Multi-domain image-to-image translation via relative attributes. In *2019 IEEE/CVF International Conference on Computer Vision (ICCV)*, pp. 5913–5921, 2019. doi: 10.1109/ICCV.2019.00601.
- Liu, X., Yoo, C., Xing, F., Oh, H., Fakhri, G., Kang, J.-W., and Woo, J. Deep unsupervised domain adaptation: A review of recent advances and perspectives. *APSIPA Transactions on Signal and Information Processing*, 05 2022. doi: 10.1561/116.00000192.
- Liu, Z., Lin, Y., Cao, Y., Hu, H., Wei, Y., Zhang, Z., Lin, S., and Guo, B. Swin transformer: Hierarchical vision transformer using shifted windows. In *2021 IEEE/CVF International Conference on Computer Vision (ICCV)*, pp. 9992–10002, 2021. doi: 10.1109/ICCV48922.2021.00986.
- Magliacane, S., van Ommen, T., Claassen, T., Bongers, S., Versteeg, P., and Mooij, J. M. Domain adaptation by using causal inference to predict invariant conditional distributions. In Bengio, S., Wallach, H., Larochelle, H., Grauman, K., Cesa-Bianchi, N., and Garnett, R. (eds.), *Advances in Neural Information Processing Systems*, volume 31. Curran Associates, Inc., 2018. URL https://proceedings.neurips.cc/paper_files/paper/2018/file/39e98420b5e98bfbdc8a619bef7b8f61-Paper.pdf.
- Manupriya, P., Das, R. K., Biswas, S., and N Jagarlapudi, S. Consistent optimal transport with empirical conditional measures. In Dasgupta, S., Mandt, S., and Li, Y. (eds.), *Proceedings of The 27th International Conference on Artificial Intelligence and Statistics*, volume 238 of *Proceedings of Machine Learning Research*, pp. 3646–3654. PMLR, 02–04 May 2024. URL <https://proceedings.mlr.press/v238/manupriya24a.html>.
- Marchezini, G. F., Lacerda, A. M., Pappa, G. L., Meira, W., Miranda, D., Romano-Silva, M. A., Costa, D. S., and Diniz, L. M. Counterfactual inference with latent variable and its application in mental health care. *Data Min. Knowl. Discov.*, 36(2):811–840, March 2022. ISSN 1384-5810. doi: 10.1007/s10618-021-00818-9. URL <https://doi.org/10.1007/s10618-021-00818-9>.
- Morioka, H. and Hyvarinen, A. Connectivity-contrastive learning: Combining causal discovery and representation learning for multimodal data. In Ruiz, F., Dy, J., and van de Meent, J.-W. (eds.), *Proceedings of The 26th International Conference on Artificial Intelligence and Statistics*, volume 206 of *Proceedings of Machine Learning Research*, pp. 3399–3426. PMLR, 25–27 Apr 2023. URL <https://proceedings.mlr.press/v206/morioka23a.html>.
- Muandet, K., Fukumizu, K., Sriperumbudur, B., and Schölkopf, B. Kernel mean embedding of distributions: A review and beyond. *Foundations and Trends® in Machine Learning*, 10(1–2):1–141, 2017. ISSN 1935-8245. doi: 10.1561/22000000060. URL <http://dx.doi.org/10.1561/22000000060>.
- Nasr-Esfahany, A. and Kiciman, E. Counterfactual (non-)identifiability of learned structural causal models, 2023. URL <https://arxiv.org/abs/2301.09031>.
- Nasr-Esfahany, A., Alizadeh, M., and Shah, D. Counterfactual identifiability of bijective causal models. In Krause, A., Brunskill, E., Cho, K., Engelhardt, B., Sabato, S., and Scarlett, J. (eds.), *Proceedings of*

- the 40th International Conference on Machine Learning, volume 202 of *Proceedings of Machine Learning Research*, pp. 25733–25754. PMLR, 23–29 Jul 2023. URL <https://proceedings.mlr.press/v202/nasr-esfahany23a.html>.
- Nguyen, K., Nguyen, D., Nguyen, Q. D., Pham, T., Bui, H., Phung, D., Le, T., and Ho, N. On transportation of mini-batches: A hierarchical approach. In Chaudhuri, K., Jegelka, S., Song, L., Szepesvari, C., Niu, G., and Sabato, S. (eds.), *Proceedings of the 39th International Conference on Machine Learning*, volume 162 of *Proceedings of Machine Learning Research*, pp. 16622–16655. PMLR, 17–23 Jul 2022. URL <https://proceedings.mlr.press/v162/nguyen22d.html>.
- Pan, Y. and Bareinboim, E. Counterfactual image editing. In *Forty-first International Conference on Machine Learning*, 2024. URL <https://openreview.net/forum?id=OXzkw7vFIO>.
- Pearl, J. *Causality: Models, Reasoning and Inference*. Cambridge University Press, USA, 2nd edition, 2009. ISBN 052189560X.
- Pearl, J. Structural counterfactuals: A brief introduction. 37 (6):977–985, August 2013. doi: 10.1111/cogs.12065.
- Poinsot, A., Leite, A., Chesneau, N., Sebag, M., and Schoenauer, M. Learning structural causal models through deep generative models: Methods, guarantees, and challenges. In Larson, K. (ed.), *Proceedings of the Thirty-Third International Joint Conference on Artificial Intelligence, IJCAI-24*, pp. 8207–8215. International Joint Conferences on Artificial Intelligence Organization, 8 2024. doi: 10.24963/ijcai.2024/907. URL <https://doi.org/10.24963/ijcai.2024/907>. Survey Track.
- Qiu, X., Rahimzamani, A., Wang, L., Ren, B., Mao, Q., Durham, T., McFaline-Figueroa, J. L., Saunders, L., Trapnell, C., and Kannan, S. Inferring causal gene regulatory networks from coupled single-cell expression dynamics using scribe. *Cell Systems*, 10(3):265–274.e11, 2020. ISSN 2405-4712. doi: <https://doi.org/10.1016/j.cels.2020.02.003>. URL <https://www.sciencedirect.com/science/article/pii/S2405471220300363>.
- Schrab, A., Kim, I., Albert, M., Laurent, B., Guedj, B., and Gretton, A. MMD aggregated two-sample test. *Journal of Machine Learning Research*, 24(194):1–81, 2023. URL <http://jmlr.org/papers/v24/21-1289.html>.
- Simonyan, K. and Zisserman, A. Very deep convolutional networks for large-scale image recognition, 2015. URL <https://arxiv.org/abs/1409.1556>.
- Sriperumbudur, B. K., Fukumizu, K., and Lanckriet, G. R. Universality, characteristic kernels and rkhs embedding of measures. *Journal of Machine Learning Research*, 12(70):2389–2410, 2011. URL <http://jmlr.org/papers/v12/sriperumbudur11a.html>.
- Teshima, T., Sato, I., and Sugiyama, M. Few-shot domain adaptation by causal mechanism transfer. In *Proceedings of the 37th International Conference on Machine Learning, ICML’20*. JMLR.org, 2020.
- Vlontzos, A., Kainz, B., and Gilligan-Lee, C. M. Estimating categorical counterfactuals via deep twin networks. *Nature Machine Intelligence*, 5:159–168, 2021. URL <https://api.semanticscholar.org/CorpusID:248986851>.
- von Kügelgen, J., Sharma, Y., Gresele, L., Brendel, W., Schölkopf, B., Besserve, M., and Locatello, F. Self-supervised learning with data augmentations provably isolates content from style. In *Proceedings of the 35th International Conference on Neural Information Processing Systems, NIPS ’21*, Red Hook, NY, USA, 2021. Curran Associates Inc. ISBN 9781713845393.
- Wang, Z., Zhang, X., and Du, H. Beyond what if: Advancing counterfactual text generation with structural causal modeling. In Larson, K. (ed.), *Proceedings of the Thirty-Third International Joint Conference on Artificial Intelligence, IJCAI-24*, pp. 6522–6530. International Joint Conferences on Artificial Intelligence Organization, 8 2024. doi: 10.24963/ijcai.2024/721. URL <https://doi.org/10.24963/ijcai.2024/721>. Main Track.
- Wu, Z., Geiger, A., Icard, T., Potts, C., and Goodman, N. Interpretability at scale: Identifying causal mechanisms in alpaca. In *Thirty-seventh Conference on Neural Information Processing Systems*, 2023. URL <https://openreview.net/forum?id=nRfClNmhVX>.
- Xia, K. and Bareinboim, E. Neural causal abstractions. *Proceedings of the AAAI Conference on Artificial Intelligence*, 38(18):20585–20595, Mar. 2024. doi: 10.1609/aaai.v38i18.30044. URL <https://ojs.aaai.org/index.php/AAAI/article/view/30044>.
- Xia, K. M., Lee, K.-Z., Bengio, Y., and Bareinboim, E. The causal-neural connection: Expressiveness, learnability, and inference. In Beygelzimer, A., Dauphin, Y., Liang, P., and Vaughan, J. W. (eds.), *Advances in Neural Information Processing Systems*, 2021. URL <https://openreview.net/forum?id=hGmrNwR8qQP>.
- Xia, K. M., Pan, Y., and Bareinboim, E. Neural causal models for counterfactual identification and estimation. In *The Eleventh International Conference on Learning*

Representations, 2023. URL <https://openreview.net/forum?id=vouQcZS8KfW>.

Yang, M., Liu, F., Chen, Z., Shen, X., Hao, J., and Wang, J. Causalvae: Disentangled representation learning via neural structural causal models. *2021 IEEE/CVF Conference on Computer Vision and Pattern Recognition (CVPR)*, pp. 9588–9597, 2020. URL <https://api.semanticscholar.org/CorpusID:220280826>.

Ye, M., Shen, J., Lin, G., Xiang, T., Shao, L., and Hoi, S. C. H. Deep Learning for Person Re-Identification: A Survey and Outlook. *IEEE Transactions on Pattern Analysis & Machine Intelligence*, 44(06):2872–2893, June 2022. ISSN 1939-3539. doi: 10.1109/TPAMI.2021.3054775. URL <https://doi.ieeecomputersociety.org/10.1109/TPAMI.2021.3054775>.

Zhang, K., Schölkopf, B., Muandet, K., and Wang, Z. Domain adaptation under target and conditional shift. In *Proceedings of the 30th International Conference on International Conference on Machine Learning - Volume 28*, ICML’13, pp. III–819–III–827. JMLR.org, 2013.

Zhang, K., Gong, M., and Schoelkopf, B. Multi-source domain adaptation: A causal view. *Proceedings of the AAAI Conference on Artificial Intelligence*, 29(1), Feb. 2015. doi: 10.1609/aaai.v29i1.9542. URL <https://ojs.aaai.org/index.php/AAAI/article/view/9542>.

Zhang, R., Isola, P., Efros, A. A., Shechtman, E., and Wang, O. The unreasonable effectiveness of deep features as a perceptual metric. In *CVPR*, 2018.

A. Appendix

A.1. Training

We use symmetric design for our work i.e. we use same architecture for both source side networks and target side networks. We use 5 hidden layers for f_θ . For context network h_ϕ , we use single hidden layer. For our noise networks, t_γ , we use 3 hidden layers. For every hidden layer, hidden dimension is 128 and every linear layer(except the last layer) is followed by PReLU (He et al., 2015). PReLU is initialized with 0.25 for f_θ , and with 0.01 for both the context and noise networks. We used skip-connections in the context network and noise network, since we observed better empirical performance using them.

We train with a dataset size of 25000. We use AdamW optimizer in stage 1 training and Adam in stage 2 training. We use linear increase followed by cosine decrease learning rate scheduler. We set the kernel hyperparameter ϱ to 1.0 throughout.